3.9 AN ANALYSIS OF A PIPE BEND SUBJECTED TO IN-PLANE LOADS

by
T. K. Hellen

This section presents results for the three dimensional finite element analysis of International Piping Benchmark Problem Number 3. The BERSAFE finite element system using both 20 node isoparametric brick elements and semiloof shell elements was used.

An Analysis of a Pipe Bend Subjected to In-Plane Loads

- by -

T K Hellen

Central Electricity Generating Board
Berkeley Nuclear Laboratories
Berkeley, Gloucestershire
United Kingdom

February 1979

SUMMARY

The report describes a set of finite element analyses conducted on a pipe bend subjected to in-plane loads. The pipe is thin-walled, and two types of finite element, shells and solid bricks, are compared elastically. An alternative semi-analytical technique has also been used and experimental results are available, all of which show good correlative agreement. The use of suitable mesh refinement and order of numerical integration is examined. Finally, the solid elements are used to follow a loading sequence incorporating elasto-plastic behaviour as conducted by experiment.

This work is an updated version of that used for the CEC benchmark calculations for the Fast Reactor Codes and Standards Working Group, Activity No 2, on Structural Analysis.

1. INTRODUCTION

The work described is the contribution from the CEGB at Berkeley Nuclear Laboratories for a benchmark calculation on the pipe elbow stress analysis proposed by Roche et al [1], which has previously been analysed experimentally and numerically. The pipe elbow geometry is shown in Fig 1 and is loaded by forces some way down the straight sections, and a key point displacement in the same direction is monitored for plotting load-displacement data, this point being approximately where the straight pipe merges with the curved section. The experiment was conducted at room temperature.

Finite element analyses have been conducted using the BERSAFE system [2]. The structure was discretized using both solid, 20 node brick isoparametric elements, and semiloof shell elements. Because of the uncertainty on the exact way the experiment was loaded, a number of load cases were considered, and the importance of using the correct numerical integration rule to evaluate the element stiffness matrices was established. A recently added facility to BERSAFE is three-dimensional plasticity and creep, and therefore the present benchmark test has been an invaluable test case for verifying the capability of this facility with the solid brick elements. Although not yet available, the plastic version of semi-loof will also be verified using such a test case.

Since the 20 node brick has 9 degrees of freedom through the shell thickness as opposed to approximately 5 in the case of typical shell elements, greater computer costs are obviously going to be incurred. But nevertheless, since the brick is the forerunner of shell elements such as the Ahmad and semiloof elements, a study of its performance in such situations is of interest. Also, the brick may be necessary in certain kinds of shell structure where portions are non-shell type attachments, eg welds.

For the present elbow problem, which has a semi-analytical solution, at least elastically, an analysis was also conducted using the program BEREL [3] which is based on a thin shell theory approach due to Rodabaugh and George [4] and the ORNL program ELBOW [5]. It produces circumferential and longitudinal stresses and strains and radial displacements at inside and outside locations around the circumference in the main symmetric plane for both in- and out-of-plane bending moments.

In addition to the experimental results of Roche et al [1], additional results from France are shown in some of the comparisons. They are the programs

TRICO [6], which performs a finite element shell analysis using triangular facet elements, and TEDEL [7], which is again based on finite elements but uses a beam-type simplified analysis.

2. THE BERSAFE FINITE ELEMENT SYSTEM

The finite element analyses all used the BERSAFE system [2]. This system has been developed as a versatile analysis aid mainly for the power industry. Initially developed for elastic analysis (Phases I and II), it has been extended to deal with plasticity and creep behaviour in arbitrary loaded structures, including steady and transient thermal effects, hardening or non-hardening materials, unloading and restart facilities, in the Phase III version [8].

The equations of equilibrium are solved by a front solution. In the plastic part of the current problem, the initial stress approach is used [9] whereby the elastic stiffness matrix is retained in an inverted state during the non-linear solution procedure, thus reducing the time of each resolution. The applied loads are applied in increments after initial yielding has occurred to follow incremental plasticity theory. Within each load increment, the alternating process of satisfying equilibrium and obeying the required yield criterion is followed until a converged condition is obtained.

A large number of different element types are available in the total system, including two and three dimensional isoparametric elements in the non-linear version. In the present example, solid brick quadratic displacement elements and semiloof shell elements were utilised for elastic comparisons, and the bricks only for the plasticity part. Stresses and plastic strains were calculated at the Gauss points where they are at their highest accuracy in each element. These points are the sampling points for the Gaussian quadratic scheme used to calculate the element stiffness matrices. Different order rules are compared.

Ancillary to the main analysis programs is a large number of programs which cover mesh generation, input data modification, file handling, results post-processing and on-line and hard-copy plotting. Interactive graphics can also be used in conjunction with the system.

3. PROBLEM DESCRIPTION

The dimensions of the geometry are shown in Fig 1. Although the actual specimen tested had variations in thickness varying from 10.5 mm to 13.1 mm round the circumference in the vertical section, labelled PR in Fig 1, it

was decided to retain a constant thickness throughout of 12 mm. The finite elements used are 20 noded hexahedral isoparametric elements, with one element through the thickness, or the semiloof shell element, which has 8 nodes and 32 degrees of freedom per element [10]. Because of symmetry considerations, a quarter of the whole structure was modelled and a typical mesh used consisted of one element through the thickness, 6 elements around the semi-circumference, and 12 rows of elements along the pipe, making 72 elements in all, as shown in Fig 2. The planes of symmetry are PQR, and ABPR, with suitably restrained degrees of freedom in those planes. The cartesian axes chosen are as shown in Fig 2, and in order to fix one node in the y direction, the outer node at location R was fixed, thereby inducing a rigid body motion in that direction. Thus, the minimum requirement of 6 fixings to prevent the 6 free rigid body motions are adequately surpassed. One loading case was repeated with 2 layers of elements through the thickness.

Further meshes were also compared during the elastic analyses. Firstly, the number of elements along the pipe was varied, keeping 6 circumferentially and one through the thickness. One such mesh was coarser, with 7 rows of elements along the pipe, whilst the other was finer, with 20 rows (Fig 3). Secondly, the number of elements circumferentially was varied, keeping 12 rows of elements along the pipe and one through the thickness. Here, 10 and 12 elements respectively, were used in place of the 6 shown in Fig 2.

The convention is used hereafter for describing the number of elements in the mesh as m x n, where m is the number of elements round the semi-circumference, and n the number of rows along the pipe, eg the mesh of Fig 1 has 6 x 12 elements.

All meshes were generated directly using automatic mesh generation programs, and the interchange of the mesh between the solid and semiloof elements was effected using an extra routine so as to retain similar node numbers at corresponding points, thereby easing the task of generating the input data and making direct comparisons of results.

The use of solid elements in such thin structures provides a useful alternative to using shell elements. The solid elements are a lot more advanced than shells and do not explicitly include shell theory assumptions. Consequently, their behaviour is inhibited neither by this nor the uncertainty prevalent in so many of the available shell elements. Their use in elastic shells has been studied many times [11], and since the non-linear version of

BERSAFE now encompasses the family of solid isoparametric elements, they were used in the plasticity study of the pipe bend. Since the stresses are evaluated at the 2 x 2 x 2 Gaussian quadrature points within each element, two such stations exist through the shell thickness so that two reference points exist for the plasticity behaviour. Since geometric non-linearities are not considered, two points are considered reasonably adequate. The semiloof element is only used for elastic analysis. It is not yet available in the plasticity version, although when it is it will be possible to investigate the effect of having different numbers of integrating points through the thickness. Its performance hitherto has been very satisfactory and may well lead to semiloof being the main shell element in use in years to come. The chief advantage of such shell elements over solid bricks is the reduction in total degrees of freedom and therefore computer costs.

Both these types of elements make use of numerical integration in evaluating their stiffness matrices, and the order of Gaussian quadrature rule has some effect on the results. Normal rules require for the 20 node brick element 27 Gauss points per elements, spaced in a 3x3x3 lattice. This is denoted as program input data as NGAUS=3. An equivalent rule which has only 13 points per element is denoted by NGAUS=13, and has consistently given almost the same results as NGAUS=3. The lesser rule NGAUS=2 (2x2x2) is theoretically insufficient for a complete integration of the stiffness matrix, but in many situations where bending effects are important, such as the present problem, it gives very accurate results, a phenomenon known as 'reduced integration'. All these rules are compared elastically. For the plasticity analysis, the NGAUS=13 rule was used with 6 semi-circumferential elements. In view of the excessive stiffness this produces, the results were adjusted to agree elastically with those of the experiment, so that the subsequent plastic deformation could be followed. The non-linear effects are not effected by the adjusted stiffness matrix. Here, the stresses are evaluated at the 2x2x2 Gauss points. The semiloof element also requires NGAUS=3, (3x3 now, since analytical assumptions are made through the thickness) for complete stiffness integration. The reduced rule is NGAUS=2, whilst a special rule with 5 points per element and denoted by NGAUS=5 is also compared.

4. LOADING SYSTEM

The applied load was effected experimentally through a system of hydraulic jacks in the normal direction to the pipe axis at the point indicated in Fig 1. A sleeved section of pipe led into the main pipe bend, of length approximately equal to AC in Fig 2. The exact form of the loading

and in particular the local bending moment applied at the loading point due to the jacking system are not known so the precise loading case to use in the finite element discretization had to be established by trial and error. Also, the exact form of the sleeve could not be modelled. In order to assess a suitable form of loading, six load cases were investigated for a particular elastic analysis, the 6 x 12 mesh of brick elements and NGAUS=13. Although this mesh and NGAUS combination gave poor results, nevertheless variations in the method of load application could usefully be compared. Because of symmetry, the load of 61000N was effectively applied as 30500 N in the program loading data. This in turn was first applied as case 1 all at one node (A in Fig 2) along -x, then in halves at nodes A and B in the same direction (case 2), then a collar load, in sevenths at each node around that semi-circumference (case 3). Case 4 was a collar load in sevenths at each node at the top of the sleeve, section CD of Fig 2, plus a bending moment to be statically equivalent to the case 3 collar loading in the section AB. This case was used by Roche et al [1] so that the sleeve section need not be discretized by finite elements, although as shown here the results from cases 3 and 4 are virtually identical, implying that case 4 implicitly assumes the sleeve to be a geometrically and materially continuous extension of the rest of the pipe. Case 5 attempted to stiffen the sleeve by doubling Young's module in that section to see if an extra bending restraint was imposed. The last case investigated the rather extreme case of zero rotation of the end section AB by restraining the y-displacement at both points A and B to zero, with no further restraints on this displacement anywhere else in the structure. Cases 5 and 6 were both loaded by the collar loading in section AB (as case 3).

Other combinations of mesh size, element type and NGAUS used the third case only (ie load applied at the vertex nodes around the semi-circumference), since little variation occurred in most of the other cases.

In particular, the plasticity runs used such a loading, and with this the sequence of the experiment was followed, first loading up to 61000N, then back to zero load, then up to 74600N, then back to zero. Then the load was restarted from 74600N to 92700N, then back to zero. Isotropic hardening was assumed. No attempt was made to model the apparent hardening of the experiment which occurred during the third load-up, and so a discrepancy there was anticipated.

For the elastic material data, Young's modulus is 191300 MPa and Poisson's ration is 0.3; these apply to the austenitic steel from Creusot-Loire of ICN 472-SP-304 type at room temperature, as used in the experiments. The non-linear stress-strain data is given in Fig 4. For BERSAFE, the non-linear data is input as points of equivalent stress against plastic strain, not total strain.

5. RESULTS

The deflection of the point measured in the experiment (point M in Fig 2) is shown for all the different cases studied in Tables 1 and 2. All analyses refer to an elastically applied load of 6100N. In the experiment, a small amount of plasticity was apparent at this load level for which a deflection of 13 mm was measured. If plasticity effects had not occurred, from the elastic slope of the load-deflection curve this deflection would have been 12.2 mms.

The effect of applying a point load (case 1) gave in all cases lower results than when either 2 or 7 nodes were loaded with 6 x 12 meshes, the difference being never more than a few percent. In the latter two cases, virtually no difference was apparent. When the loading was applied at the top of the sleeve (case 4), the results were almost identical to those of case 3. This loading consisted of a -x force totalling 30500N in section CD, plus a couple applied as y-forces at points C and D in Fig 2 to be statically equivalent to case 3 (-x force in section AB). This technique was used by Roche et al [1] to avoid modelling the sleeve, but, as shown here, implicitly assumes the sleeve is a smooth extension of the pipe. The effects of doubling Young's modulus for the sleeve (case 5) gave a small but insignificant drop in the displacements. However, when the end was restrained from rotation, by prescribing the y-displacements of points A and B to zero, the measured deflection was reduced from 7.113 mm to 1.255 mm, showing a tremendous restraint on the deformation behaviour of the whole pipe bend. This case is clearly inappropriate.

These results demonstrate that the case 3 loading is suitable for general use, and thus has been applied to all the other meshes. Fig 5 shows the measured deflection as a function of the number of elements in the semi-circumference, for both types of element and integrating rule used. In all cases, 12 elements along the pipe were used. The reduced integration (NGAUS=2) cases agree very well with the experimental elastic result of 12.2 mms, irrespective of the number of semi-circumferential elements. This is frequently true of reduced integration, and the good accuracy extends to the stresses as well as the displacements. For the complete integrating rules, the brick (NGAUS=13) is

seen to converge much more slowly than the loof elements (NGAUS=3). Invariably the NGAUS=13 results are almost identical to NGAUS=3 in the bricks, so the former is preferred because of less computer cost.

The effect of varying the number of rows of elements along the pipe in the solid element meshes, 6x7, 6x12 and 6x20, shows virtually no difference in the main calculated displacement, despite the low value produced by using NGAUS=13. Also, the 6x12 mesh was repeated with 2 layers of elements through the thickness, and again no significant change was observed. Consequently, the important mesh design parameter for this type of structure is the number of circumferential elements.

The deformed outside surface of the pipe in the main symmetry plane (plane PQR of Fig 2) is shown in Fig 6 for the brick elements at the elastic load level 6100N. The BEREL [3] results use a semi-analytical approach and so produce a deformation which tends to a sinusoidal shape. The four sets of finite element results compare both 6 and 12 semi-circumferential elements, each with complete and reduced integration. The two sets of reduced integration results are identical, within the thickness of the plotted line. The complete rule with 12 semi-circumferential elements gives a similar deformation, the three curves being less smooth than the semi-analytical result due to second order effects which are not picked up by the latter method.

The corresponding deformations for the semiloof elements are shown in Fig 7. Again, the reduced integration rules and the NGAUS=3 12 semi-circumferential element case produce curves similar to the semi-analytical method, although now the two reduced integration results are no longer identical. As in Fig 6, the 6 element, NGAUS=3 case produces insufficient deformation.

For the solid elements mesh of 6x12 elements, elastic load case 3, and NGAUS=2, the strains in the pipe cross-section UV, inclined at 45^{o} to the y-axis (Fig 2), are shown in Figs 8 and 9. Fig 8 shows axial strains at the inner, mid and outer surfaces and are compared with measure experimental strains (presumably on the outer surface) and results using the TRICO program [6] and the TEDEL program [7]. Fig 9 shows the circumferential strains in the midsurface. Overall agreement in each case is good, bearing in mind the difficulty in measuring experimental strains accurately and their relative inaccuracy in the finite element method.

For the elasto-plastic analysis, the load-deflection curves of the measured point M of Fig 2 are shown in Fig 10 for the complete loading history. Agreement with the experimental results is good up to load level 7460ON. The

unloading is different due to the slight difference in elastic slope between the two approaches. However, in the absence of any form of kinematic hardening in the present analysis, it was found that unloading followed by a reloading to the same load produced no difference to the results there, so the second unloading and reload at load 74600N was ignored. The final path to load 92700N showed a slope consistent with that below the 74600N level, as would be expected. However, the experimental results show a distinct return of slope to that of elasticity at this point, showing some kinematic hardening effect not picked up by the program. The final unloading gives a close permanent distortion between the two approaches.

A re-analysis of the elasto-plastic case with a more suitable combination of mesh refinement and integrating rule is shortly to be undertaken.

CONCLUSIONS

Finite element analyses have been conducted on a pipe bend subjected to in-plane loads. The analysis requires a three-dimensional discretisation but because of the thinness of the pipe walls, shell elements have also been used. Consequently the opportunity has been taken to compare solid brick isoparametric elements with semiloof shell elements. Several different mesh refinements were attempted, and the quality of results was only affected by the number of elements circumferentially. In particular, only one element through the thickness was required. The effect of using different numerical integrating rules for stiffness matrix evaluation was studied. The use of reduced integration has been shown to greatly enhance the quality of results. For the brick element, a special 13 point rule is shown to give almost identical results to the complete 3x3x3 rule, which requires 27 points per element. Several load cases were tried, including the number of loaded nodes round the loaded circumference, the effect of stiffened sleeves, another loaded circumference plus a corrective couple, and a severe pipe end restraint. Little difference resulted in all cases except the latter, where a drastic decrease in the measured deflection occurred.

Cross-sectional deformation plots show a substantially good agreement between the elastic finite element results and those produced from the semi-analytical program.

In the elasto-plastic analysis, the elastic stiffness matrix was adjusted to agree with the experimental stiffness. The load-deflection curves at the measured point of the experimental test have been reproduced quite well by the finite element program using the solid elements, the main discrepancy being due to a hardening effect observed in the experiment in the final part

of the loading but which could not be incorporated in the non-linear data used in the finite element analysis.

ACKNOWLEDGEMENTS

The author expresses his gratitude to Mrs V Flack for her invaluable assistance in conducting the various computations, to the Central Electricity Generating Board for permission to publish, and to R Roche of Centre d'Etudes Nucléaires de Saclay, France, for permission to use the French results.

REFERENCES

1. Roche, R, Vrillon, B and Brouard, D, 1978, "Room Temperature Elastic Plastic Response of a Thin Walled Elbow Subjected to In-Plane Bending Loads", Current Benchmark Submission.

2. Hellen, T K and Protheroe, S J, 1974, "The BERSAFE Finite Element System", Comp. Aided Design, Vol 6, No 1, pp 15-24.

3. Beveridge, D, 1975, CEGB Report RD/B/N3244.

4. Rodabaugh, E C and George, H H, 1957, "Effect of Internal Pressure of Flexibility and Stress-Intensification Factors of Curved Pipe or Welding Elbows", Trans ASME 79, 939-48.

5. Dodge, W G and Moore, S E, 1973, "ELBOW - A Fortran Program for the Calculation of Stresses, Stress Indices and Flexibility Factors for Elbows and Curved Pipes", ORNL-TM-4098.

6. Hoffman, A and Jeanpierre, F, "Program TRICO: Analyse des Structures Tridimensionnelles Composées de Coques et de Poutres", CEA-N-1930 Note, CEN, Saclay.

7. Hoffman, A et al, "Program TEDEL", CEA Note, Saclay.

8. Hellen, T K and Harper, P G, 1976, CEGB Report RD/B/N3597.

9. Zienkiewicz, O C, Valliapan, S and King, I P, 1969, "Elasto-Plastic Solutions of Engineering Problems - The Initial Stress Finite Element Approach", Int J Num Meth Eng'g, 1, 75-100.

10. Irons, B M R, 1975, "The Semiloof Shell Element", Dept Civil Eng. Research Report CE75-5, Univ Calgary.

11. Hellen, T K, 1971, CEGB Report RD/B/N2087.

TABLE 1 Measured Displacements for Elastic Load λ = 61000N for Various Runs

Meshes with Brick (20 Node) Elements

Run	Mesh (mxn)	Integrating Rule	Load Case	Displacement (mm)	Computer Cost (units of £1)
1	6x12	13	1 pt load	6.980	
2		13	2 pt loads	7.112	77.61
3		13	7 pt loads	7.113	
4		13	Loading above sleeve	7.114	
5		13	Stiffened sleeve	7.097	
6		13	Zero rotation below sleeve	1.255	
7		2x2x2	1 pt load	11.844	
8		2x2x2	2 pt loads	12.233	72.18
9		2x2x2	7 pt loads	12.239	
10		3x3x3	1 pt load	6.984	
11		3x3x3	2 pt loads	7.116	96.14
12		3x3x3	7 pt loads	7.117	
13	6x7				44.63
14		13	7 pt loads	7.002	
15		2x2x2	7 pt loads	12.218	40.15
16	6x20	13	7 pt loads	7.119	130.51
17		2x2x2	7 pt loads	12.244	118.86
18	Double Layer 2x6x12	13	7 pt loads	7.125	
19	10x12		11 pt loads	10.556	149.40
20	12x12	13	13 pt loads	11.283	215.44
21	12x12	2x2x2	13 pt loads	12.220	202.52

TABLE 2 Measured Displacements for Elastic Load λ = 61000N for Various Runs Meshes with Semiloof Shell Elements

Run	Mesh	Integrating Rule	Load Case	Displacement (mm)	Computer Cost (units of £1)
1	6x12	3x3	1 pt load	8.554	
2		3x3	2 pt loads	8.782	47.60
3		3x3	7 pt loads	8.783	
4		2x2	1 pt load	12.526	
5		2x2	2 pt loads	12.930	42.41
6		2x2	7 pt loads	12.926	
7		5	1 pt load	11.512	
8		5	2 pt loads	11.886	44.73
9		5	7 pt loads	11.885	
10		3x3	7 pt loads	8.920	
11	6x20	3x3	7 pt loads	9.796	
12	6x12	3x3	6 pt loads	9.065	57.13
13	6x12	3x3	7 pt loads	9.065	57.04
14	10x12	3x3	11 pt loads	11.387	78.84
15	10x12	2x2	11 pt loads	12.738	70.83
16	12x12	3x3	13 pt loads	11.893	
17	12x12	2x2	13 pt loads	12.666	91.41

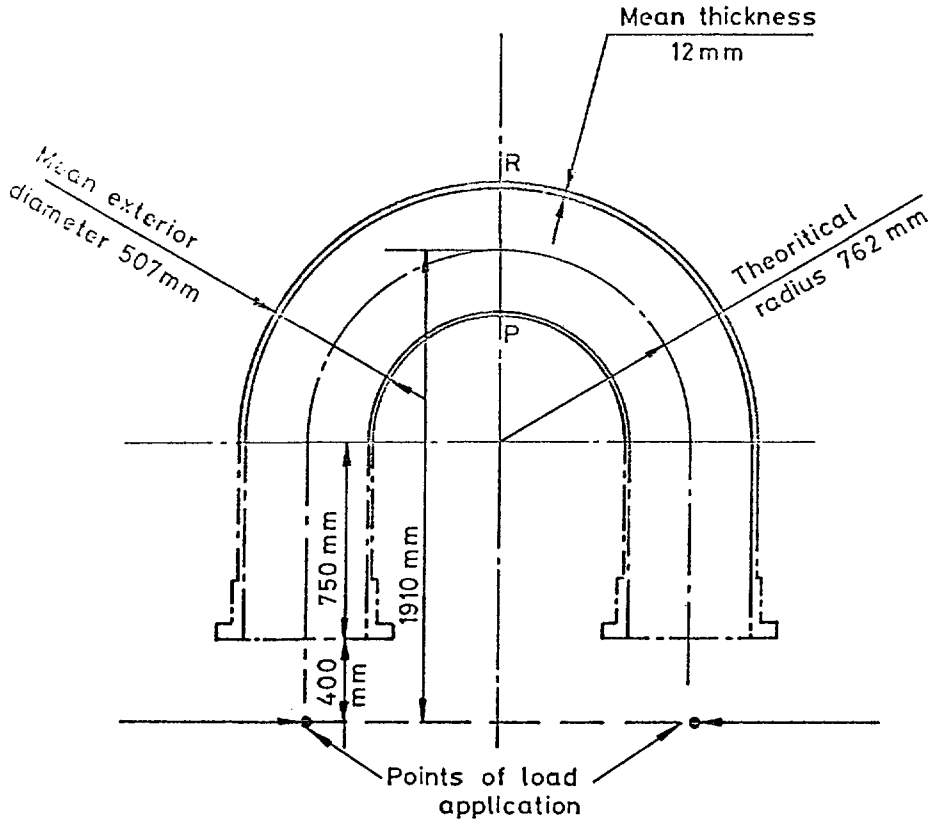

FIG. 1. Geometry of Pipe Bend.

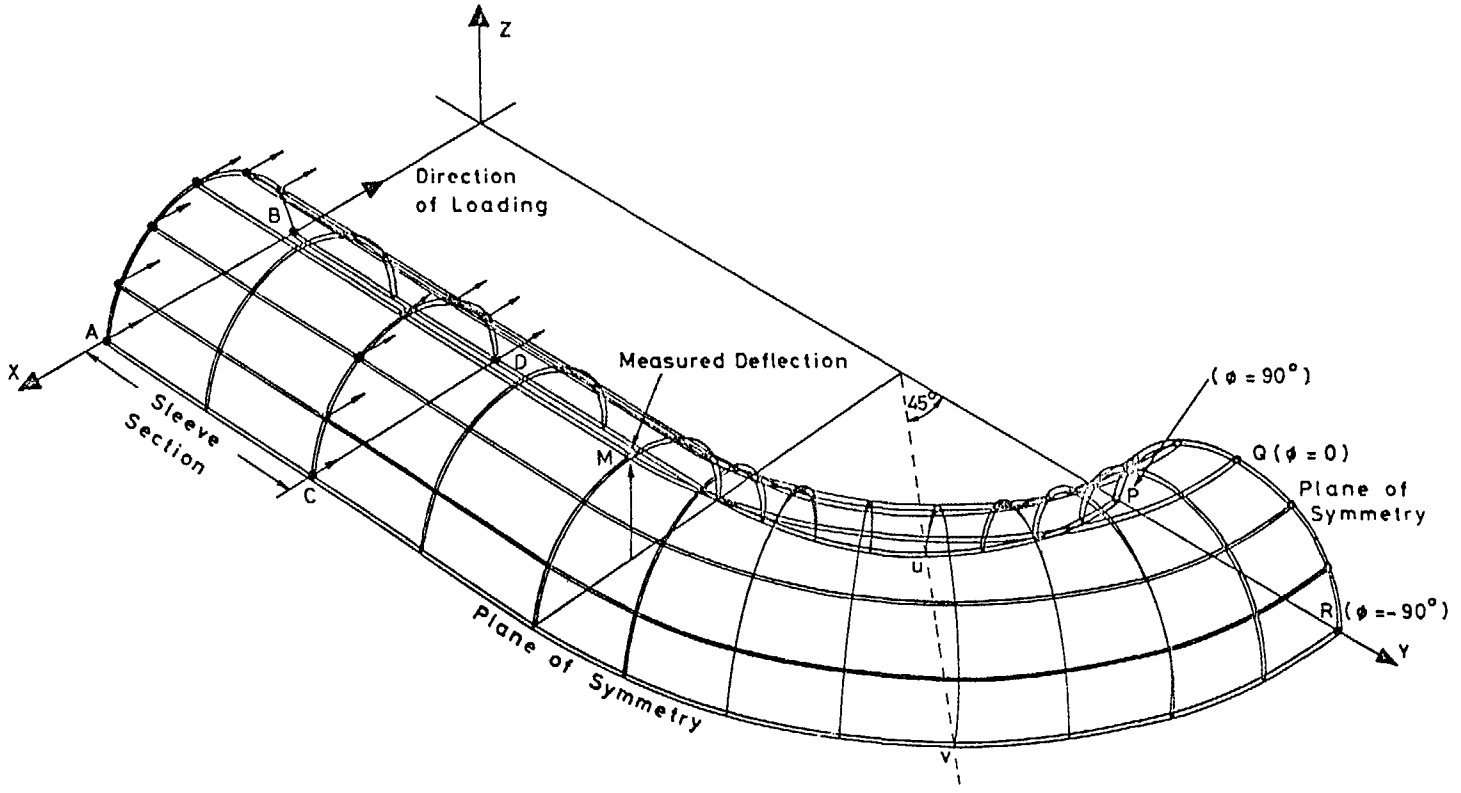

FIG. 2 Finite Element Discretization of Pipe Bend (Medium Mesh)

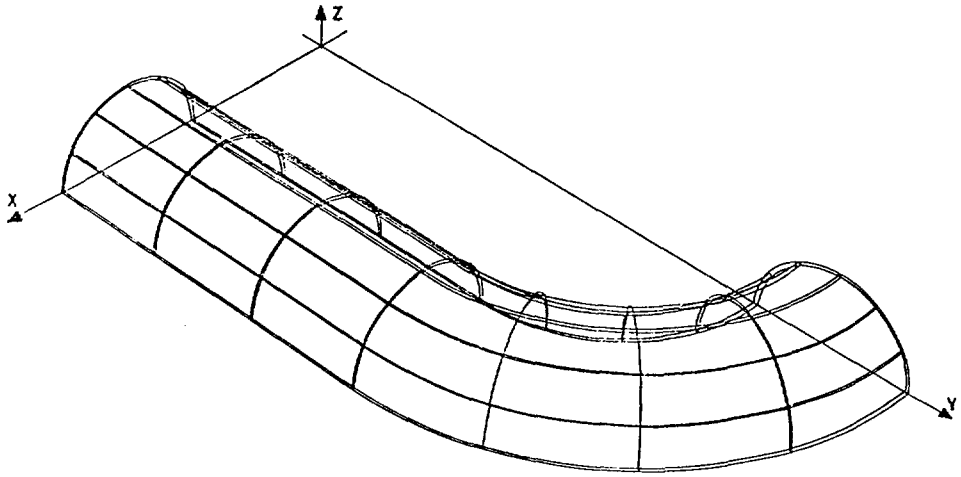

Coarser Mesh of 6 x 7 Elements

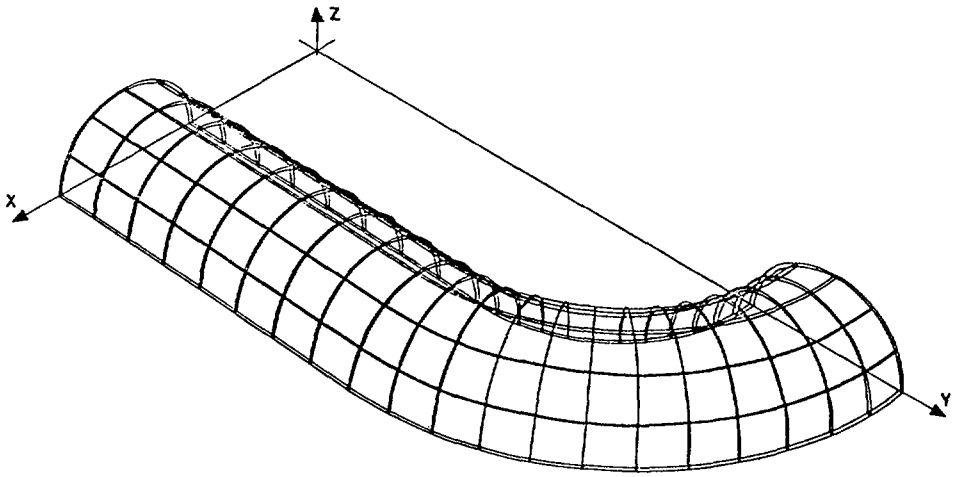

FIG. 3 Finer Mesh of 6 x 20 Elements.

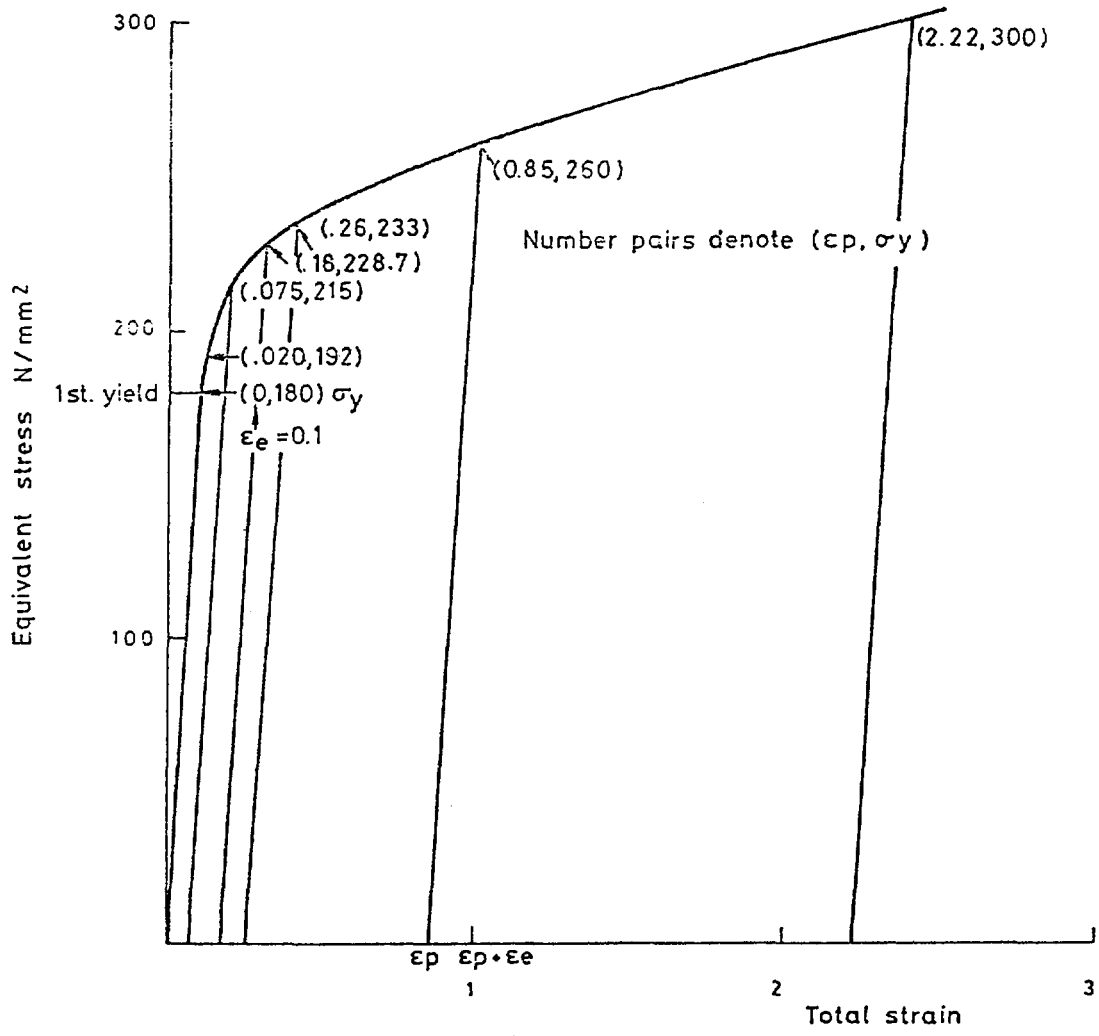

FIG.4. Non-Linear Data for Pipe Bend.

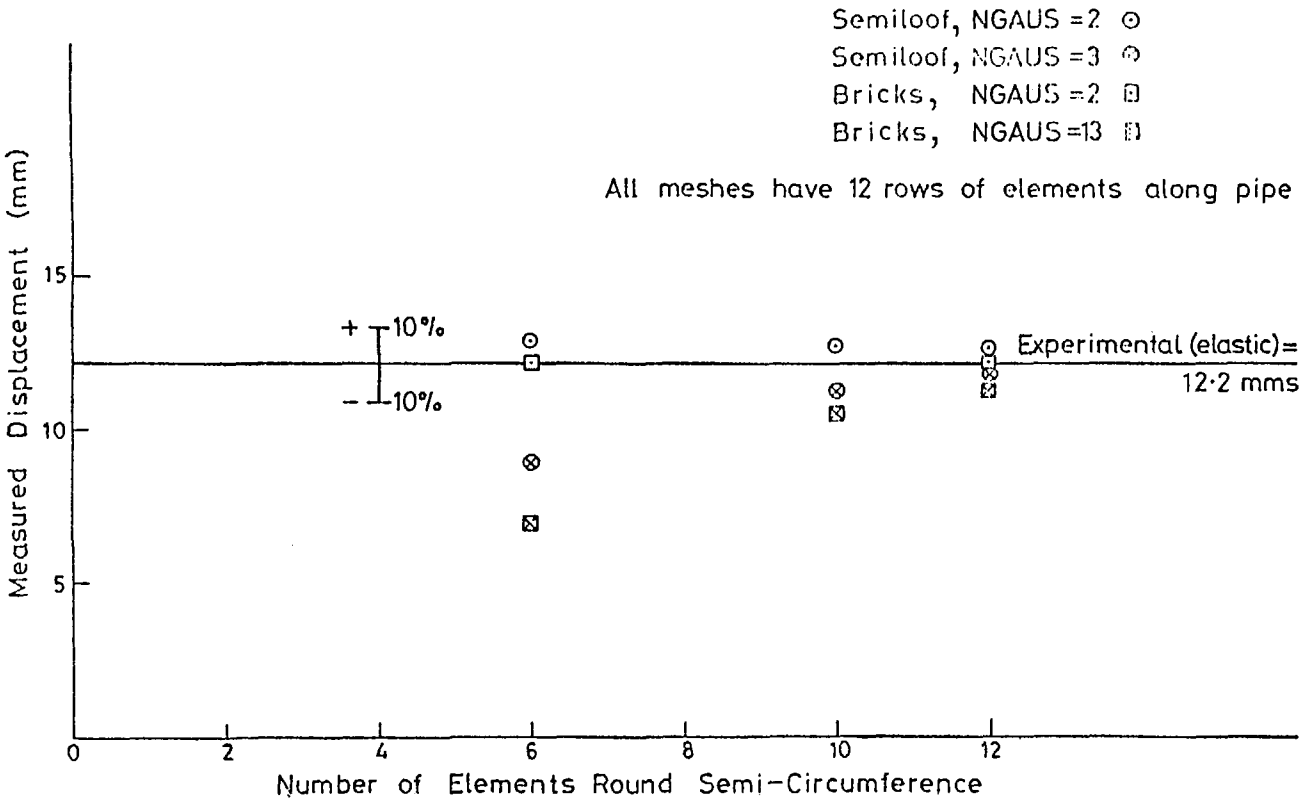

FIG. 5. Measured Point Displacements for Different Meshes, Elements and NGAUS.

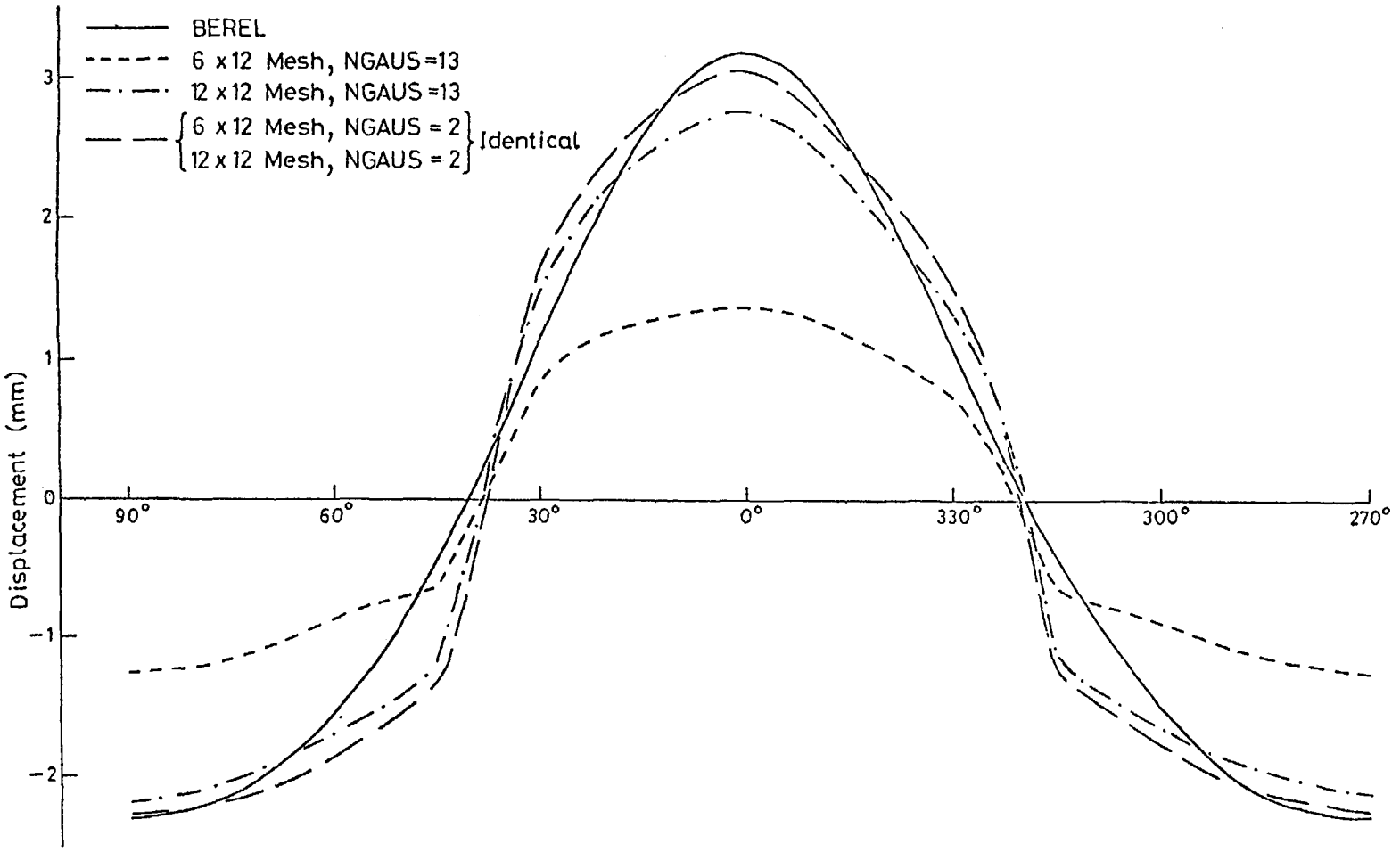

FIG. 6. Radial Displacements Around Outside Surface in Symmetry Plane X=0 for Brick Elements. Load = 61000N, Elastic Conditions.

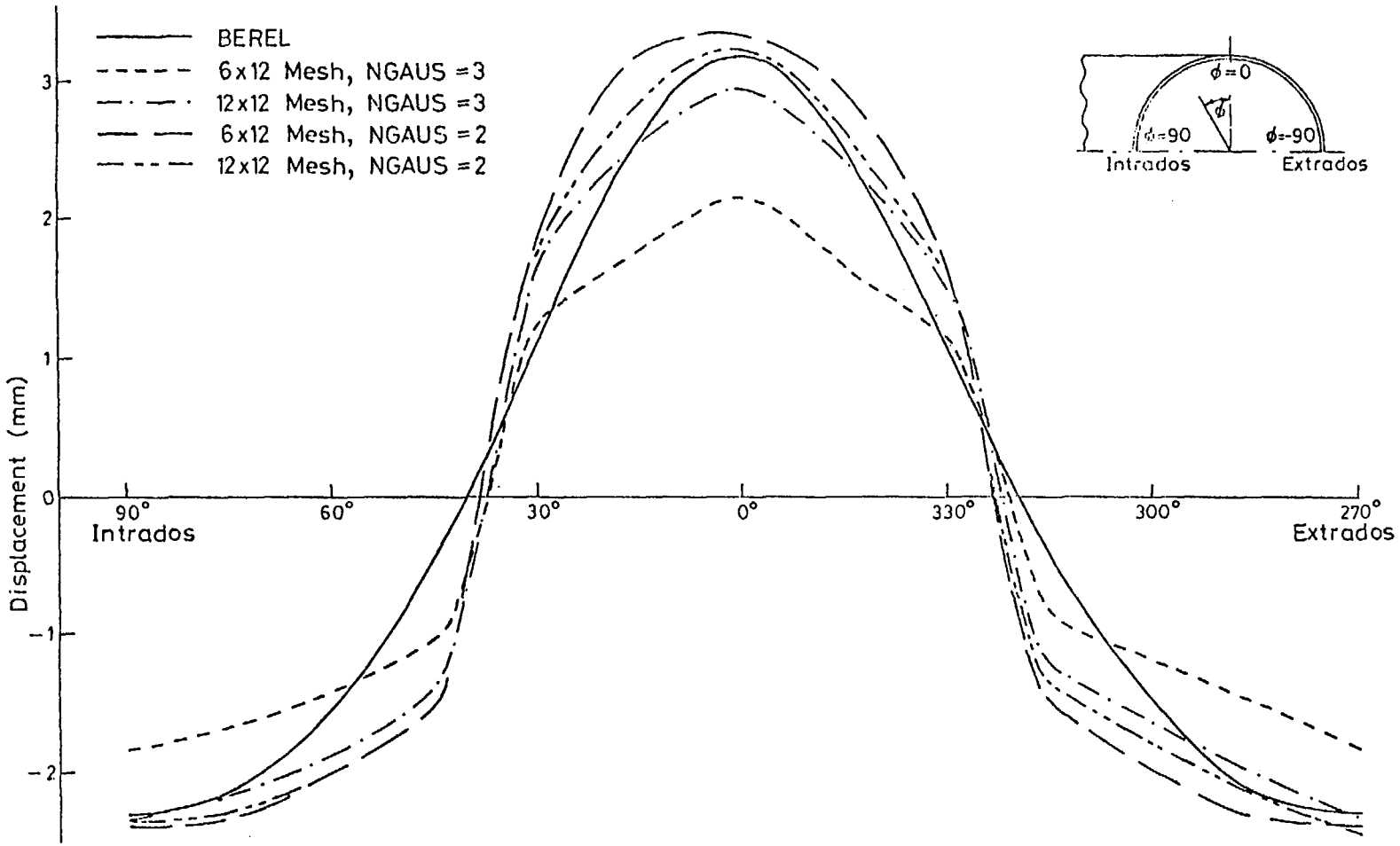

FIG. 7. Radial Displacements Around Mid Surface in Symmetry Plane X=0 for Loof Elements. Load = 61000 N, Elastic Conditions.

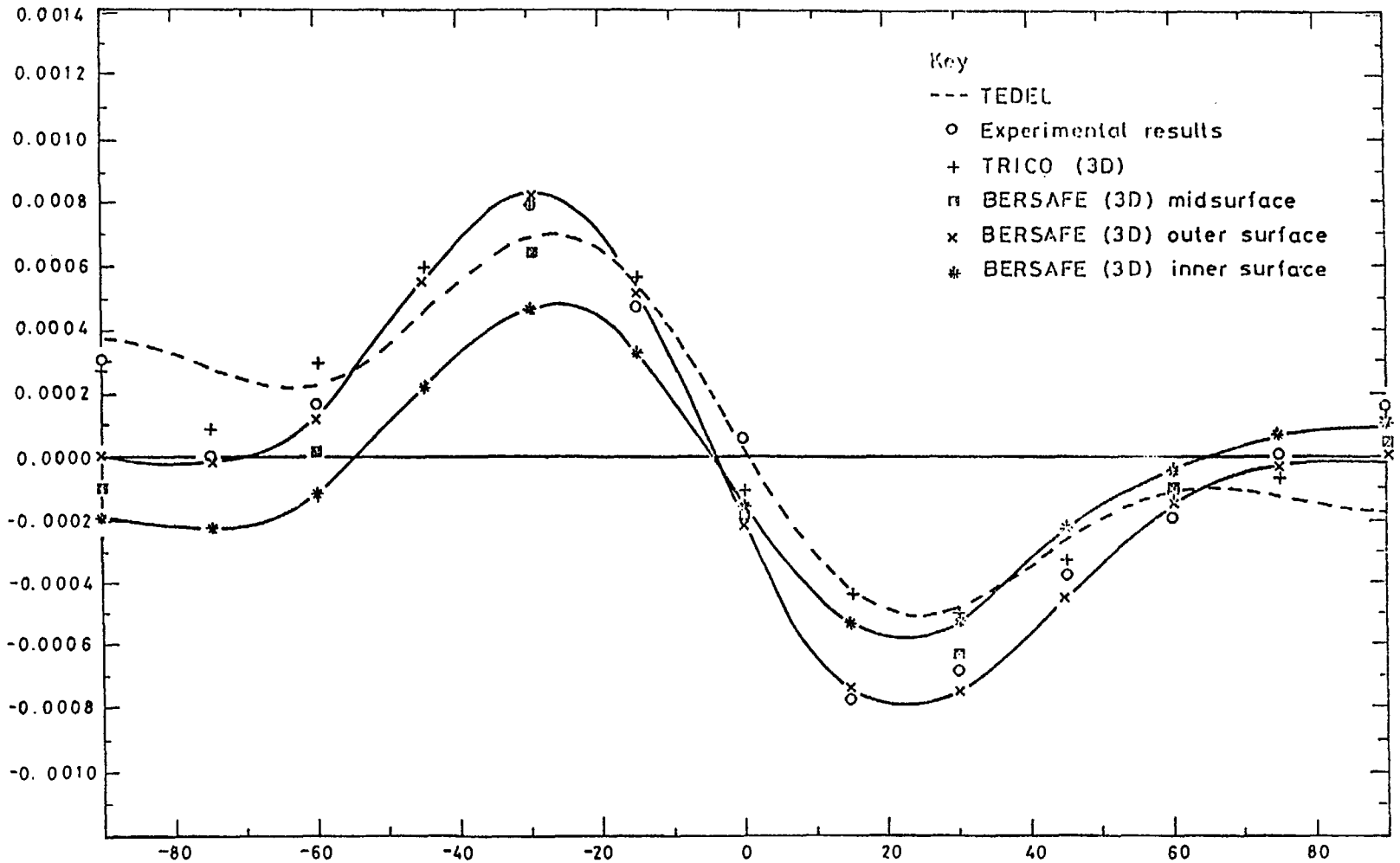

FIG. 8.

Axial strains for load = 61000N, with 6 circumferential EZ60 elements and NGAUS = 2 strains obtained using plopper

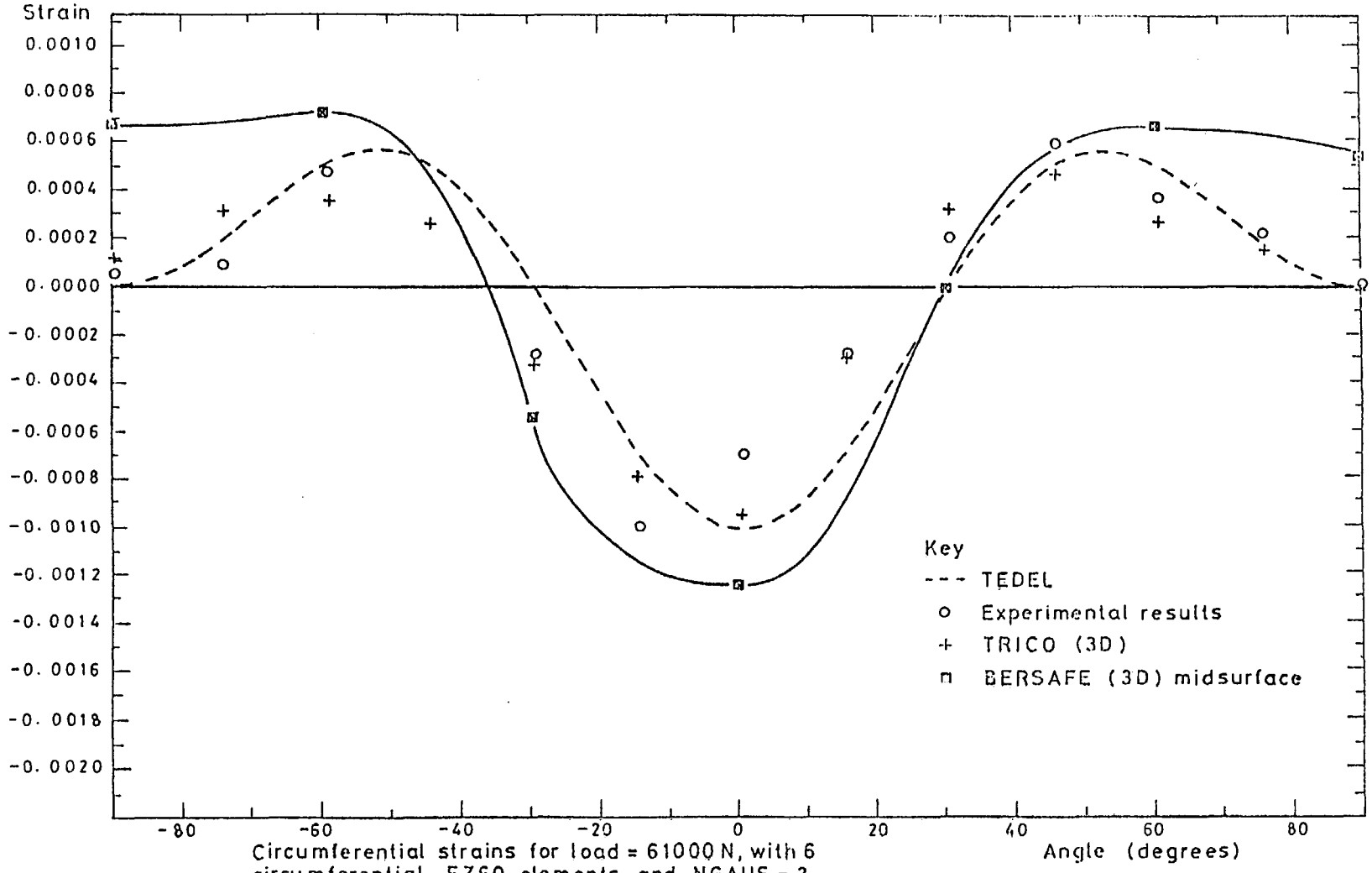

FIG. 9. Circumferential strains for load = 61000 N, with 6 circumferential EZ60 elements and NGAUS = 2 strains obtained using plopper.

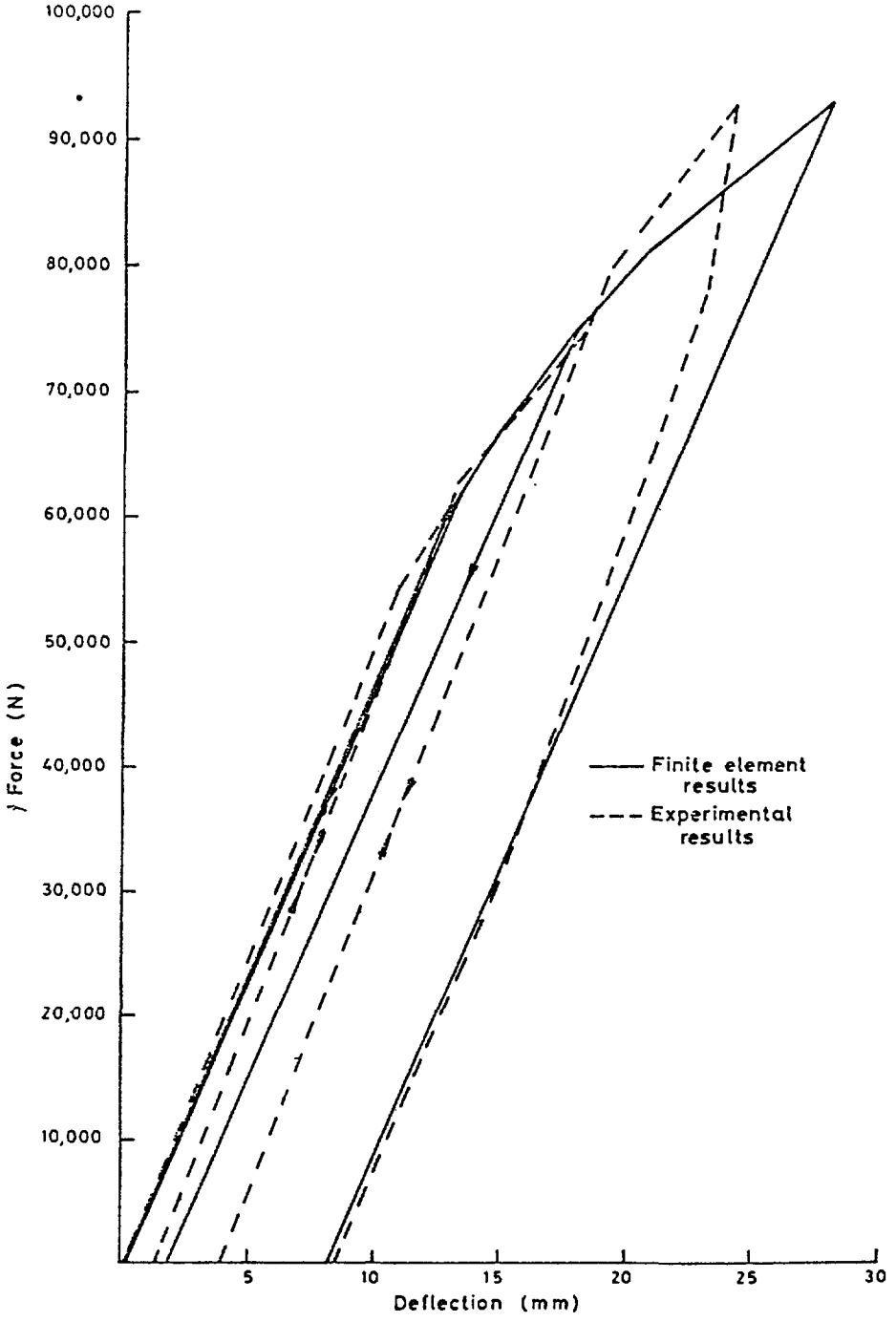

FIG.10. Load - Deflection Curves.